© Indian Academy of Sciences

Water discharge and suspended sediment dynamics in the Chandra River, Western Himalaya

Ajit T Singh[1,2,*] , Parmanand Sharma[1], Chirag Sharma[2], C M Laluraj[1], Lavkush Patel[1], Bhanu Pratap[1], Sunil Oulkar[1,2] and Meloth Thamban[1]

[1]*National Centre for Polar and Ocean Research (NCPOR), Ministry of Earth Sciences, Vasco-da-Gama, Goa 403 804, India.*
[2]*School of Earth, Ocean and Atmospheric Sciences, Goa University, Goa 403 206, India.*
Corresponding author. e-mail: ajit.t.singh@gmail.com

Glacier systems are important components of the hydrological cycle and a major source of meltwater and sediment flux that controls the river ecology, water quality, and hydropower generation in the Indian Himalayan Region (IHR). Thus, understanding short- and long-term changes in water and suspended sediment (SS) dynamics is crucial in highly sensitive pro-glacial Himalayan Rivers. In the present study, the Chandra River basin in Western Himalaya was chosen to study river discharge, SS transport dynamics, physical erosion rate, and their governing factors for the 2017 melting season (May–September). The daily mean water discharge and SS concentration in the Chandra River was 260.7 m^3s^{-1} and 775.5 mgL^{-1} with maximum discharge and SS flux in the month of July. The air temperature showed significant relationship with the river discharge ($R^2 = 0.67$; $n = 156$; $p < 0.001$), which in turn controlled the SS export in the basin ($R^2 = 0.86$; $n = 130$; $p < 0.001$). An anticlockwise sediment-discharge hysteresis during peak flow conditions suggest exhausted sediments or large distance of sediment transport (>100 km) from the upper glacierized region to the end of the basin. Statistical analysis of SS particle size showed poorly sorted immature grains with a dominance of silt particles (85%), followed by sand (8.5%) and clay (6.5%). The SS estimates revealed a total suspended sediment yield of 1285 tons km^{-2} yr^{-1} and physical erosion rate of 0.47 mm yr^{-1}. Considering the socio-economic importance of the Himalayan region, the present study will help to evaluate the water and sediment budget of the Chandra River, Western Himalaya and to establish their relationship to the meteorological conditions in the basin.

Keywords. River discharge; suspended sediment; hysteresis loop; grain size; Chandra River; Western Himalaya.

1. Introduction

Himalayan glaciers are shrinking in the recent decades, generating an increased volume of meltwater and as a result, increased transportation of suspended sediment (SS) flux (Immerzeel *et al.* 2012; Milner *et al.* 2017; Mao *et al.* 2019). The Indus, Ganga, and Brahmaputra river basins together contribute ∼6–10% of global sediment influx to the ocean, resulting in the buildup of world's two largest submarine fans in the Arabian Sea and the Bay of Bengal (Subramanian 1993). Amount of SS flux in a river directly affects its water quality, which is necessary for sustaining river ecology, agriculture, hydropower, and drinking water in the downstream region (Haritashya

et al. 2006; Wulf *et al.* 2012; Kumar *et al.* 2018). The sediment budget of the Himalayan rivers greatly varies owing to various factors such as energy conditions, availability of sediments, topography, snow cover, and meteorological conditions (Chakrapani and Saini 2009; Haritashya *et al.* 2010; Iida *et al.* 2012; Kumar *et al.* 2016). Additionally, various studies have shown that the water and sediment flux from the glaciated catchments may significantly alter as a result of climate change (Wulf *et al.* 2012). Therefore, it is crucial to understand the long-term and short-term dynamics of hydrology and sediment export from highly sensitive glacierized regions (Mao *et al.* 2019).

The SS flux in the Himalayan rivers is mostly comprised of sand (0.06–1.00 mm), silt (0.002–0.06 mm) and clay (<0.002 mm) size particles, controlled by energy conditions and availability. The grain size of SS significantly affects various downstream processes. Increase in silt size particles makes agricultural land more productive. However, they also increase the turbidity of water which reduces permeability to dissolved gases, nutrients, affecting the primary productivity and macro-invertebrate communities (Davies Colley and Smith 2001; Descloux *et al.* 2013; Bona *et al.* 2016). A study by Bona *et al.* (2016) showed that the benthic invertebrates are more sensitive to fine sediments and thrive well in the presence of coarse sediments. The increasing magnitude of SS also affects the hydropower projects in the Himalayan rivers as the water quality degrades, and finer sediments result in siltation of dams and abrasion of hydropower turbines (Dharmadhikary 2008; Arora *et al.* 2014).

Despite the hydrological and socio-economic importance of Indian Himalayan Region (IHR), small numbers of studies have been conducted to estimate water and sediment budget of the proglacial streams and rivers of IHR (Rao *et al.* 1997; Haritashya *et al.* 2010; Arora *et al.* 2014; Kumar *et al.* 2016; Kumar *et al.* 2018; Singh and Ramanathan 2018). The major challenges in studying the Himalayan rivers are due to poor accessibility, high elevation, undulated terrain, logistic difficulties and harsh weather conditions in the region. In this paper, the Chandra River situated in the upper Indus Basin, Western Himalayan region was studied for 2017 melting season (May–September) with an aim to understand short (daily) and long-term (monthly) changes in river water discharge (Q), SS fluxes and to establish their relationship to meteorological conditions.

2. Study area and geology

The present study was conducted in the Chandra River basin which is one of the major glacierized basins in the Western Himalaya. The total basin area is $\sim$2440 km^2, out of which about 30% (703 km^2) is occupied by glaciers (Tawde *et al.* 2017) (figure 1). The basin elevation extends from 2800 to 6600 masl with a mean slope of 21$^{\rm o}$. The Chandra River emerges from the Bara Lacha region, which is further joined by other snow and glacier-fed tributaries downstream. The river flows for $\sim$125 km from its point of origin to its confluence with the Bhaga River at Tandi forming the Chandra–Bhaga River, a major tributary of the Chenab River of the Indus river system (Rao *et al.* 1997) (figure 1). The precipitation in the study region is derived partly from the Indian Summer Monsoon (ISM) and Western Disturbances (WD's) where the WD contribute predominantly (>70%) to the precipitation in the form of snow during November–April (Dimri *et al.* 2015; Pratap *et al.* 2019; Singh *et al.* 2019). Major runoff contribution to the Chandra River is governed by the seasonal snow and glacier melt from major glaciers like Bara Shigri, Samudra Tapu, Sutri Dhaka, Batal, Chhota Shigri and Hamtah, which are under retreating phase over the last few decades (Azam *et al.* 2014; Patel *et al.* 2016; Sharma *et al.* 2016; Tawde *et al.* 2017). The vegetation in the basin is sparse because of semi-arid to arid conditions. The steep slope, high contribution of glacier meltwater and narrow valley of the Chandra Basin makes it a suitable place for hydropower generation. Hence, many future hydropower plans have been proposed in the basin with a potential power capacity of $\sim$1125 MW (https://sandrp.files.wordpress.com).

Geologically, the Chandra Basin lies in the central crystalline zone of the Pir-Panjal Range of the Indian Himalaya. The geology of the basin is diverse and majorly comprises of rocks ranging from Proterozoic (2500–542 ma) to Cenozoic era (66 ma to present) (Kumar *et al.* 1987). Rocks in this basin are composed of meso to keto-metazonal migmatites, metamorphites, gneisses and recent sediment deposits. The basement rocks are composed of granite, gneiss, and granitoid rocks from the proterozoic era, which is overlained with rocks from Haimanta group after a tectonic break (Kumar *et al.* 1987; Geological Survey of India (GSI) 2011). The Haimanta group of rocks is mainly composed of slates, phyllites, quartzite, and fine-grained biotite-schists (Kumar *et al.* 1987).
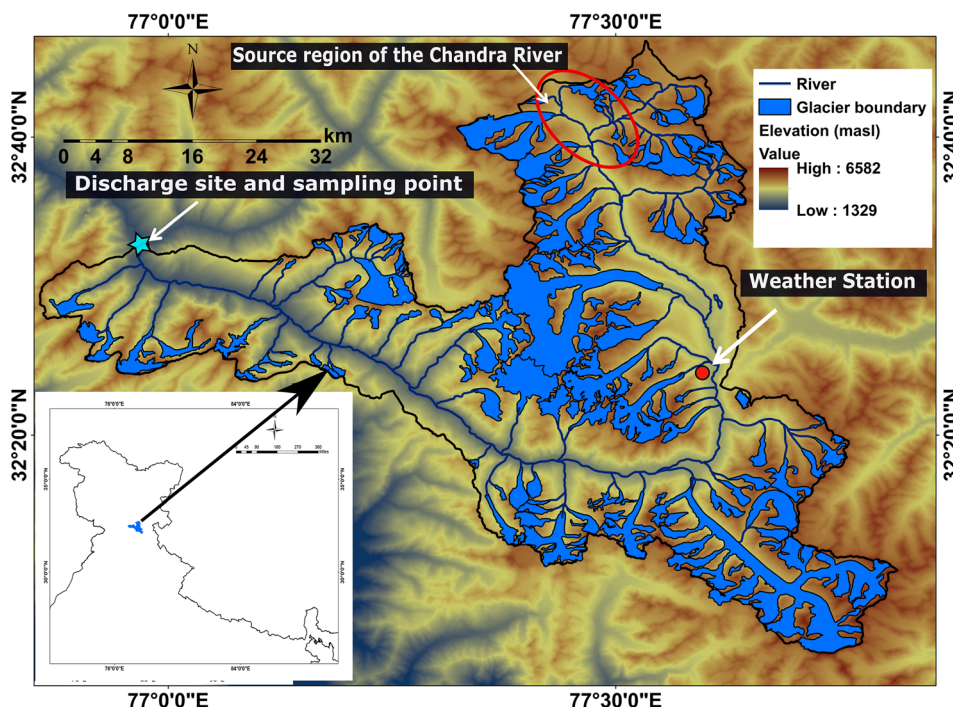
Figure 1. Chandra River basin drainage and glaciers with the location of automatic weather station (AWS), discharge site and sampling location.

Most recent deposits are of glacial, alluvial, and fluvial origin resulting in the formation of moraines, hillwash, scree, and riverbank deposits. The detailed geology and lithology of the study region are provided in figure 2 and table 1.

3. Material and methods

Meteorological observations such as daily air temperature, relative humidity and precipitation were monitored using an automatic weather station (AWS, Campbell Scientific) installed at the Himansh Base Camp (HBC) in the Chandra Basin (4080 masl) (figure 1). The AWS equipped with the automated air temperature sensor (Campbell HC2S3, range: − 50 to +60°C; accuracy: ± 0.1°C), precipitation bucket (OTT Pluvio Model, range: 0–1800 mm/hr; accuracy: ± 0.05 mm) and data logger (Campbell Scientific–CR1000) were used for continuous data measurement and logging at 10-min interval. A hydrological station was established at Tandi towards the end of the Chandra Basin (catchment area of 2440 km^2 up to the gauging site) for discharge measurement and twice-daily water sampling (at 8:00 and 17:00 hrs) was made (figure 1). For collecting the hydrological data during 2017 melting season, the continuous water level in the river was recorded at every 10 sec interval using a YSI radar sensor (Nile series) with storm data logger having ±2 mm accuracy. The discharge of the Chandra River was computed using the area-velocity method. Excessive velocities, depth, and rolling boulders at the river bed prohibited us from using current meter and depth profiler for velocity measurements. Hence, the surface velocity of the river was determined at different parts using wooden float whereas the depth of the river was measured by using gauging rod (Haritashya *et al.* 2006; Srivastava *et al.* 2014; Kumar *et al.* 2016, 2018; Singh *et al.* 2017). After calculating the river discharge, a stage (water levels) *vs.* discharge relationship (rating curve) was established (figure 3). The discharge measurement of Himalayan stream and river involves inherent uncertainties associated with gauging the depth and measuring stream velocity. Previous studies in the Himalayan region have shown that the area-velocity based discharge estimate of Himalayan rivers involves an uncertainty of ∼5–10% (Haritashya *et al.* 2006; Srivastava *et al.* 2014; Kumar *et al.* 2016). In our study, the fitting curve of stage *vs.* discharge relationship has an accuracy of ±6%, which demonstrates the reliability discharge estimation. However, the bed topography of the Himalayan streams and rivers changes constantly, and regular monitoring of river cross-section is hazardous in furious high altitude rivers.
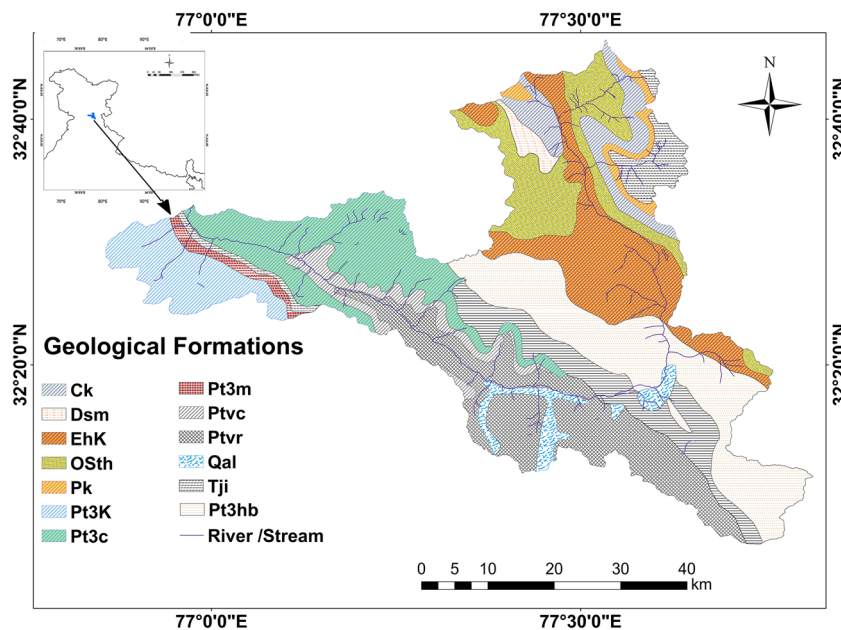
Figure 2. Geological formation and mineral map of the Chandra River basin in Western Himalaya modified after available geology and mineral map of Himachal Pradesh provided by Geological Survey of India (GSI (2011) Geological and Mineral Map of Himachal Pradesh. Source: www.gsi.gov.in).

Table 1. *Geological formations of the Chandra River basin and the mineral composition modified after available Geology and Mineral map of Himachal Pradesh provided by Geological survey of India (GSI (2011) Geological and Mineral Map of Himachal Pradesh. Source: www.gsi.gov.in).*

Era	Age	Name	Formation	Group	Composition
Cenozoic	Quaternary	Qal	Fluvial/Fluvio-Glacial/Alluvial	–	Moraines, hillwash, scree
Paleozoic	Triassic to Jurassic	TJI		Und. Lilang Group	Shale, dolomite and limestone
	Carboniferous to Permian	PK, Ck		Und. Lilang Group	Shale, sandstone
	Devonian	Dsm	Muth Formation	Senugba Group	Quartz arenite and slate
	Ordovician to Devonian	Osth	Thango Formation	Haimanta Group	Quartz arenite and shale
	Cambrian	EhK	Kunzamla Formation	Haimanta Group	Slate, phyllite, siltstone, limestone
	Neo-Proterozoic	Pt3k	Katargill Formation		
Proterozoic		Pt3m	Manjir Formation		Siltstone, slate, conglomerate, and limestone
		Pt3c	Chamba Formation		Schist
		Pt3hb	Batal Formation	Haimanta	Slate, phyllite, quartzite, schist
		Ptvc	Cholathach Formation	Vaikrita Group (Central Crystalline)	Granite, gneiss, and granatoids

To measure the SS concentration, we carried out high-frequency (i.e., twice daily at 08:00 and 17:00 hrs) water sampling at the discharge site (figure 1) during May–September 2017 in pre-cleaned 500 ml HDPE bottles. Similarly, to understand the diurnal pattern in river discharge and SS dynamics, water and sediment samples were collected on a bi-hourly basis for 24 hrs on the selected day of each month (May–September). The water samples were immediately filtered onsite using 0.45 μm cellulose membrane filter paper to separate SS particles. Thereafter, the samples were properly cased and
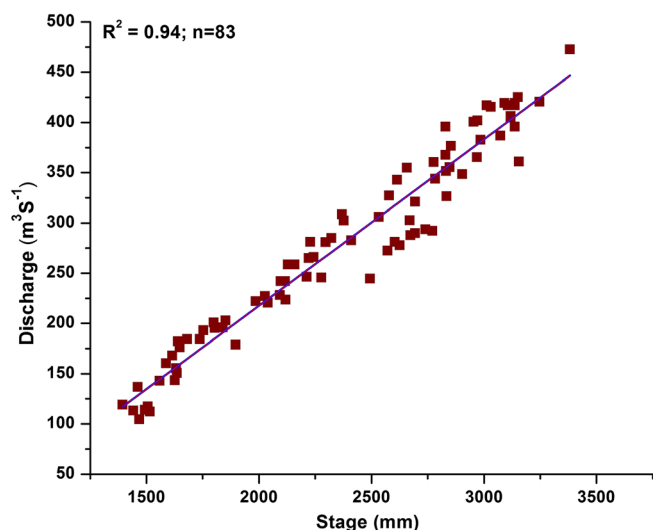
Figure 3. The Chandra River stage-discharge relationship at Tandi to estimate the discharge during melting season (May–September 2017).

transported back for further laboratory analysis. The suspended sediment concentration (SSC), suspended sediment load (SSL), suspended sediment yield (SSY), erosion rate (E_{ss}) and grain size characteristics of monthly bulk SS were estimated after post-weighing the filter paper (Udden 1914; Folk and Ward 1957; Kumar *et al.* 2016). Because of frozen conditions, the winter months (October–March) contributed a negligible amount of meltwater and SS flux from the glacierized areas to the downstream region. Therefore, the present study was considered only for melting/ablation season (May–September).

The snow cover area of the Chandra Basin (April–September 2017) was analyzed using the MODIS/Terra Snow Cover Daily L3 Global 500 m grid (MOD10A2) snow cover products available at 500 m spatial resolution with eight-day interval (Hall and Riggs 2016). The detailed description of the MOD10A2 dataset is provided in the NSIDC website (https://nsidc.org/). The obtained tiles were further processed for the Chandra Basin using ArcGIS 10 environment.

4. Results and discussion

The daily mean air temperature at the Himansh Base Camp ranged from −5.1 to 13.4°C with a daily mean of 7.6°C. The mean monthly air temperature for May, June, July, August and September were 2.9, 7.4, 11.9, 10.8, and 6.5°C, respectively (figure 4a). The snow-cover in the

Chandra Basin varied from 2347 to 987.1 km^2 during April–September. During early spring (April–May), the entire basin was covered with winter snow (October–March) (figure 4b). In early spring, followed by summer, the winter snow melted and contributed to the river discharge. Therefore, a good relationship was observed between daily mean air temperature, snow cover and discharge in the Chandra Basin (figure 4). The daily mean discharge during the study period varied from 115 to 457 m^{3}s^{-1} with an overall mean of 260.7 m^{3}s^{-1}. The daily mean discharge for May, June, July, August and September were 196, 259, 394, 306, and 160 m^{3}s^{-1}, respectively (figure 4c). The total precipitation reported in the Chandra Basin during 2017 ablation season was 206.3 mm. The monthly rainfall for May, June, July, August and September at Himansh were 41.6, 57.4, 25.7, 18.3, and 63.3 mm, respectively. Major precipitation events occurred in the month of May, June, and September while July and August months showed relatively lower precipitation amount (figure 4d).

The SS concentration in the river is mainly a function of discharge, snow cover, and temperature (table 2). The daily mean SSC ranged from 308.9 to 1943.1 mgL^{-1} with a mean of 775.5 mgL^{-1} (figure 5). A significant correlation was observed between mean daily discharge and SSC ($R^2 = 0.86$; $n = 130$; $p < 0.001$) which is attributed to the influence of varying energy conditions of river discharge on SSC (figure 5a and b). Mean monthly SSC for May, June, July, August and September were 533.8, 685.4, 1125.8, 1071.9, and 527.2 mgL^{-1}, respectively. The mean monthly relationship between discharge and SSC concentration of the Chandra River remained similar to a daily mean relationship. Since temperature is the major governing factor for the discharge, it also showed a good relationship with the SS concentration ($R^2 = 0.64$; $n = 130$; $p < 0.001$) (figure 5c and d). A significant positive correlation among temperature, discharge and SS also suggests an increase in mobilization of stored sediment by the glaciers during previous winter and sediment along the river as the glacier melt raises the river discharge with an increase in temperature during summer (May–September). Similarly, Rao *et al.* (1997) also reported a strong correlation between sediment and discharge of the Chandra River ($R^2 > 0.8$). A strong relationship between SS and discharge has also been demonstrated in other Western Himalayan rivers such as Wanger, Baspa and Sutlej
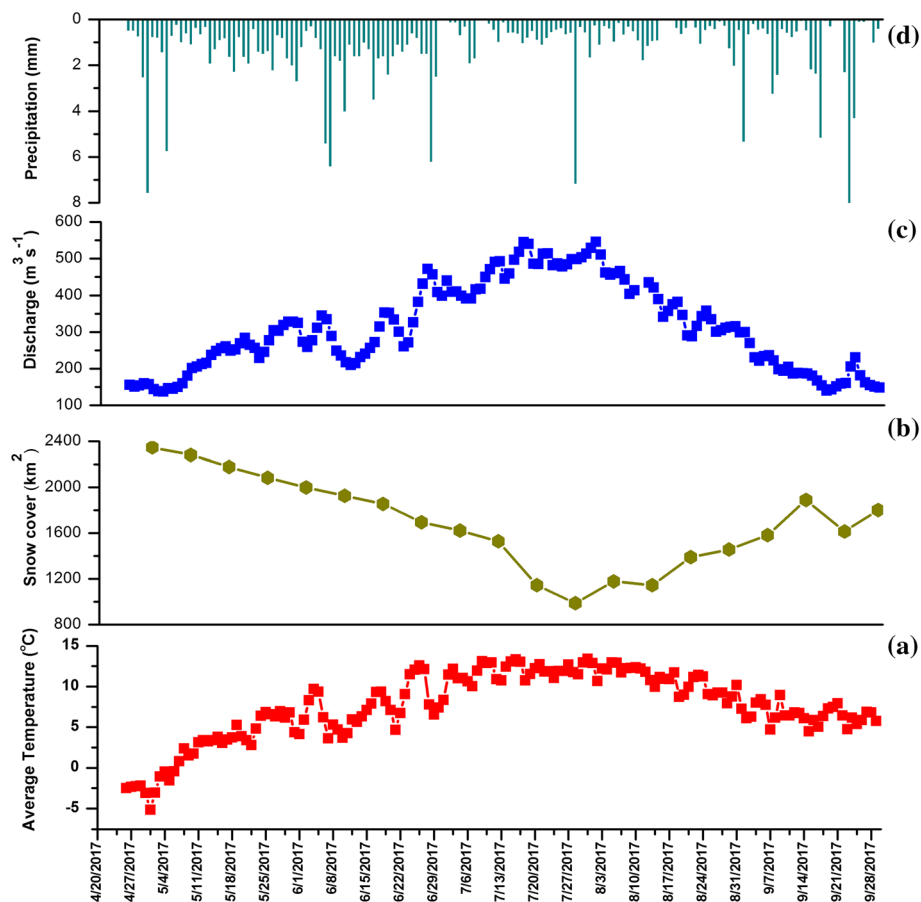
Figure 4. Daily distribution of (**a**) air temperature, (**b**) snow cover, (**c**) daily discharge, and (**d**) precipitation for the Chandra River basin during the 2017 melting season (May–September).

Table 2. *Statistical distribution of different hydrometeorological datasets and suspended sediment for the 2017 melting season (May–September).*

Parameters		May	June	July	August	September	May–September
Temp (°C)	Mean	3.0	7.4	12.0	10.9	6.5	7.7
	SD	3.0	2.6	1.2	1.4	1.1	4.2
	CV	1.01	0.34	0.10	0.13	0.16	0.54
Discharge (m^3s^{-1})	Mean	196.6	259.1	394.4	306.2	160.4	260.7
	SD	51.3	60.9	36.8	71.6	33.0	99.6
	CV	0.26	0.23	0.09	0.23	0.20	0.38
SSC (mgL^{-1})	Mean	533.8	685.4	1125.8	1072	527.3	775.6
	SD	136.5	190.8	297.8	305.1	275.6	362.0
	CV	0.25	0.27	0.26	0.28	0.52	0.46
Total Meltwater Flux (MCM)	Mean	526.4	671.6	1060.4	820.1	415.6	3536.7
Total SSC load (tons)	Mean	27.7×10^4	49×10^4	121×10^4	92.1×10^3	23.5×10^4	313×10^4
Suspended sediment yield (tons km^{-2})	Mean	113.7	200.8	496.2	377.5	96.3	1284.6
Erosion rate (mm yr^{-1})	Mean						0.47

River (Wulf *et al.* 2012) suggesting similar hydrological characteristics in snow and glacier dominated (nivo-glacial) regimes. A good correlation of SS with discharge also suggests that the SS in the Western Himalayan rivers is predominantly controlled by transport energy, unlike precipitation amount in the monsoon dominated regimes (Kumar *et al.* 2016).

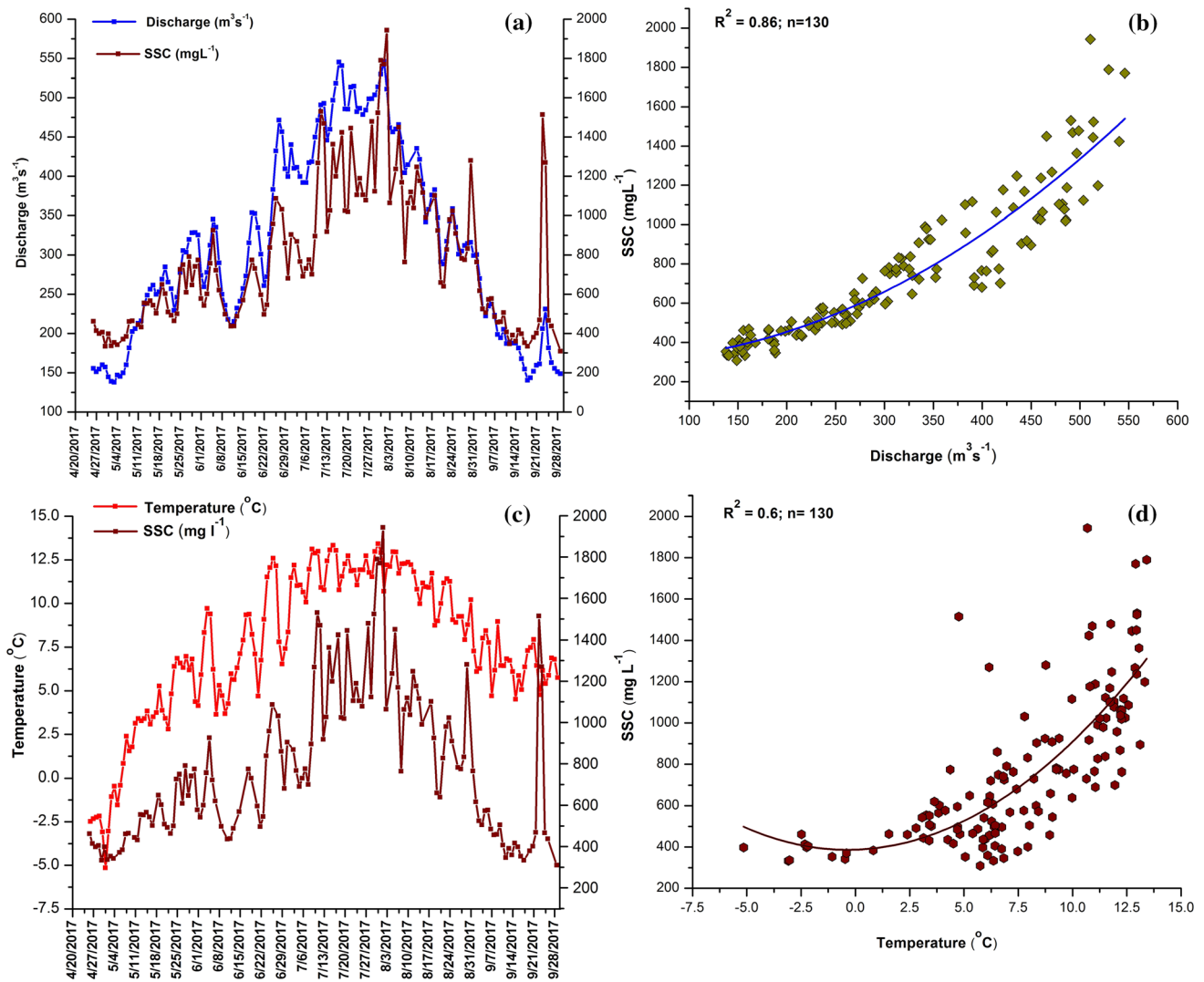A poor relationship ($R^2 < 0.1$) was observed between daily rainfall events and SSC. Since the

Figure 5. Daily mean variation of SSC in relationship with discharge (**a**, **b**) and temperature (**c**, **d**) observed in the Chandra Basin, Western Himalaya during 2017 melting season (May–September).

rainfall was mostly in the form of drizzles, no significant change in sediment export were observed during the rainfall events. However, lack of immediate response of sediment export during rainfall could also be due to the delay factor that occurs in the larger catchments like the Chandra Basin. A strong negative correlation was observed between snow cover and SSC ($R^2 = 0.87$; $n = 17$; $p < 0.001$) from May to mid-August, which diminishes as the snow cover depletes and discharge starts declining with drop in temperature (figure 6). Since the entire Chandra Basin area is snow-covered in the month of April, and as the snow melting commences in the early May, it mobilizes the sediment in the basin, raising SSC concentration. As the temperature increases, the melting of snow progresses until the snow cover reaches the equilibrium line altitude (ELA)

($\sim$5200 masl) (Tawde *et al.* 2017). Most of the winter snowpack were melted by the end of July and thereafter the major contribution of meltwater and SS were sourced from glacier discharge.

The proportion of discharge and SSC from the basin varied significantly on a monthly basis. May and June received 34% of total runoff and transported 24.5% of the total sediment load. About 54% of the total runoff was received in July and August and transported 68% of the total sediment. Whereas, September contributed only 12% to the total discharge and transported 7.5% of the total sediment load. Coefficient of variance (CV) of daily SSC for May, June, July, August, and September was 0.25, 0.27, 0.26, 0.28, and 0.52. A substantial increase in the CV of SSC for September month could be due to a drastic drop in the SSC during the latter half of the month due to lack in the
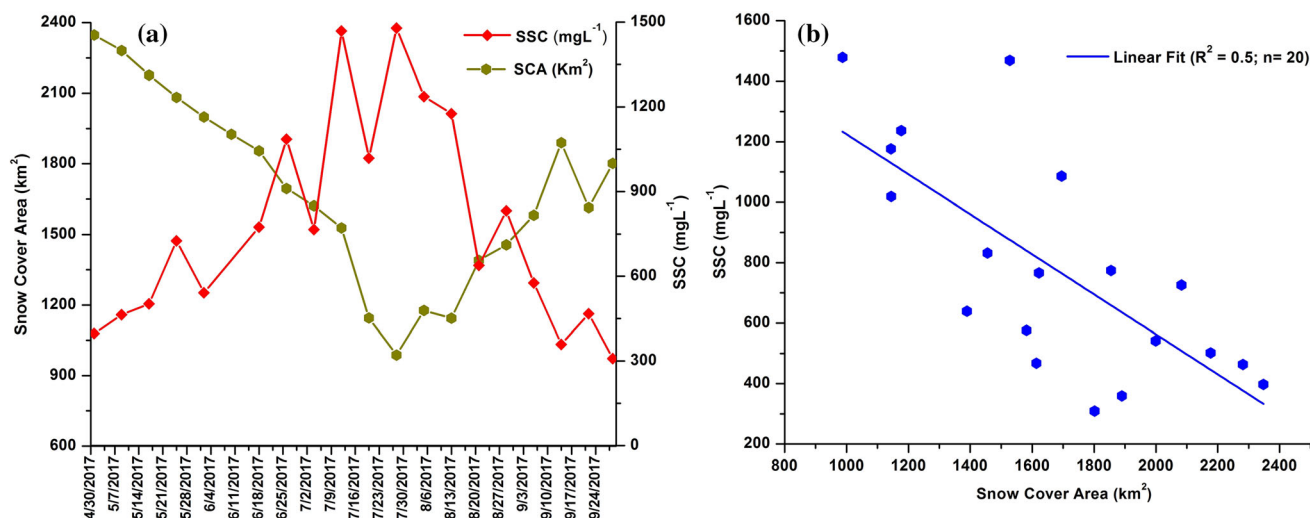
Figure 6. (**a**) Daily mean of snow cover area and suspended sediment concentration and (**b**) relationship between mean daily snow cover area and suspended sediment concentration (May–September 2017) observed in the Chandra Basin, Western Himalaya.

availability of sediment and significant drop in discharge. The CV for monthly discharge for May, June, July, August and September were 0.26, 0.23, 0.09, 0.23, and 0.20, respectively (table 2). A major change in the CV of discharge in July (0.09) could be due to the transition from snowmelt to glacier-melt contribution to the river, where winter snow cover diminishes and a major contribution with stable discharge is delivered by the glacier melt. The overall (May–September) CV for SSC and discharge was 0.46 and 0.38. The daily SS load (SSL) in the Chandra River varied from 3.3×10^3 to 72×10^3 tons day^{-1}. The daily mean of SSL for May, June, July, August and September were 9.7×10^3, 16×10^3, 39×10^3, 29×10^3, and 7.8×10^3 tons day^{-1}, respectively. The mean monthly SS Yield (SSY) during the months of May, June, July, August and September was 113.8, 200.8, 496.2, 377.5, and 96.3 tons km^{-2}, respectively (figure 7 and table 2). Since the discharge contribution beyond these months is considered to be $< 10\%$ and SSC reduces significantly during lean flow conditions, it can be stated that the SSY for the complete year is ~ 1285 tons km^{-2} yr^{-1}.

The estimated SSY of the Chandra Basin is significantly higher than the average global SSY (~ 150 tons km^{-2} yr^{-1}) and the Indian subcontinent (~ 327 tons km^{-2} yr^{-1}) (Jha *et al.* 1988). A previous study (Rao *et al.* 1997) of the Chandra River (from 1978 to 1995) shows an average sediment yield of 513 tons km^{-2} yr^{-1}, suggesting a nearly two-fold higher sediment yield in the present study. The estimated modern erosion rate of the Chandra Basin in the present study is 0.47 mm

yr^{-1}. Previous literature has shown a rapid retreat in glaciers of the Chandra Basin resulting in $\sim 18\%$ overall increase in water loss (Tawde *et al.* 2017). Also, 67% loss of low altitude glaciers were reported in the Chandra Basin from 1984 to 2012 (Tawde *et al.* 2017). This may have significantly raised the discharge and in return increasing the SSC, SSY and erosion rate of the Chandra Basin. The overall discharge and SS flux during the study period were 3536 Million Cubic Meters (MCM) and 3 million tons, respectively. A study conducted by Singh and Ramanathan (2018) on the Chhota Shigri Glacier in the Chandra Basin showed a higher SSY of ~ 3000 tons km^{-2} yr^{-1}. Higher denudation rate at the Chhota Shigri Glacier is potentially attributed to higher physical denudation due to closeness of study site at the glacier snout and higher altitudinal variation. Similarly, Singh *et al.* (2014) also reported much higher SSY (~ 7663 tons km^{-2} yr^{-1}) in the upstream region of the Gangotri Glacier, Central Himalaya influenced by the steepness of the river gradient, and integrated effect of the heavy rainfall from Indian Summer Monsoon (ISM) and glacier affected physical erosion (Kumar *et al.* 2016). However, downstream regions of the Ganga Basin at Alaknanda and Bhagirathi River showed reduced SSY of 863 and 907 tons km^{-2} yr^{-1} as the intensity of glacier influenced physical erosion reduces in the downstream region (Chakrapani and Saini 2009). Almost similar SSY of 865 tons km^{-2} yr^{-1} were reported for downstream region of the Brahmaputra Basin (Subramanian 1996). The erosion rate for Nepal Himalayas was reported between 0.1 and 2.8
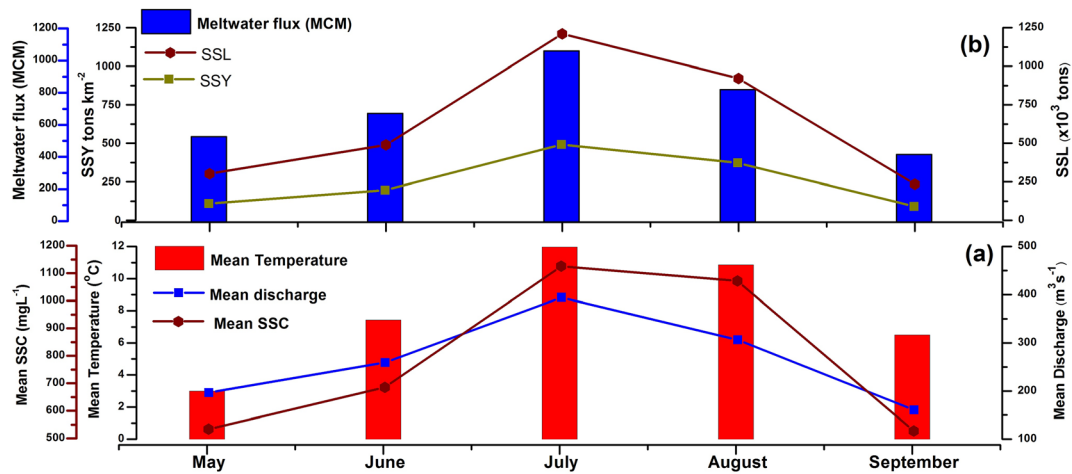
Figure 7. (**a**) Monthly mean temperature, discharge and suspended sediment concentration and (**b**) Meltwater flux, suspended sediment load and suspended sediment yield from the Chandra River (May–September 2017).

mm yr^{-1} with relatively lower rates (< 0.5 mm yr^{-1}) for higher Himalayas (Andermann *et al.* 2012). The spatio-temporal variability in the amount of precipitation is one of the significant factors governing SSY and erosion rate across the Himalayan belt. A study conducted by Bookhagen *et al.* (2005) in Baspa Basin, Western Himalaya showed significant increase in mean erosion rate from $\sim 0.7 \pm 0.14$ to 1.5 mm yr^{-1} triggered by abnormally higher monsoonal rain. Besides precipitation, variability in exhumation rate of rocks across the Himalayan belt showed an influence on the physical erosion, generating the variable amount of SS (Fort 2000).

The bi-hourly data collected on selected days representative of each month during May–September revealed significant fluctuation in temperature, SSC and discharge. Our data revealed that the daily maximum temperature ($T_{\max}$) for selected diurnal days was reported at 1200–1600 hrs and maximum discharge ($Q_{\max}$) was reported at 2200–2400 hrs for selected days. A delayed response of discharge with respect to temperature showed mean lag time $\sim$6–8 hrs, which could be due to the delayed routing of meltwater from snow/glaciers to the discharge site.

At a short term scale (hourly), the sediment-discharge relationship is often non-linear showing variable trend during ascending and descending limb resulting in a hysteresis loop (Mao *et al.* 2019). Sediment-discharge hysteresis loops are frequently used to understand the sediment dynamics and transport processes. A typical clockwise hysteresis is a result of readily available SS material. In the present study, most of the hysteresis reveal an anticlockwise hysteresis with a

heterogeneous pattern (non-linear) for lean discharge months, while the clear anticlockwise pattern for July and August diurnal days (high flow conditions) (figure 8c and d). Similarly, the monthly mean discharge and SSC shows an anticlockwise hysteresis suggesting a clear pattern on long term period (figure 8f). A clear anticlockwise hysteresis during July and August indicates exhaustion of the sediments due to open hydrological network in the glacierized region as the temperature and discharge increases (Tananaev 2015). Additionally, anticlockwise hysteresis could also be a result of long distance sediment transport from the upper glacierized region of the basin to the sampling point at the end of the basin. Considering the maximum number of glaciers in the upstream region, the erosion process and supply of sediment to the discharge site could be delayed by several hours. Based on the short term sediment availability during the lean discharge period, the basin showed heterogeneous/complex hysteresis characteristics. Heterogeneous hysteresis in glacierized region is due to low efficiency of the hydrological system during the early ablation period as the melt water is mostly sourced from the snow cover (figure 8a, b, and f) (Mao *et al.* 2019). During the initial melting period (April–May), snow cover obstructs the supra-glacial, subglacial and englacial drainage from the glacierized region. As the winter-deposited snow in the basin melts away, a major source of the meltwater is derived from the well-routed glacier melt showing a clear Q-SSC hysteresis. However, as the temperature drops in September, it results in refreezing and melting of the glacier melt resulting in less efficient water routing from the basin (Łepkowska and
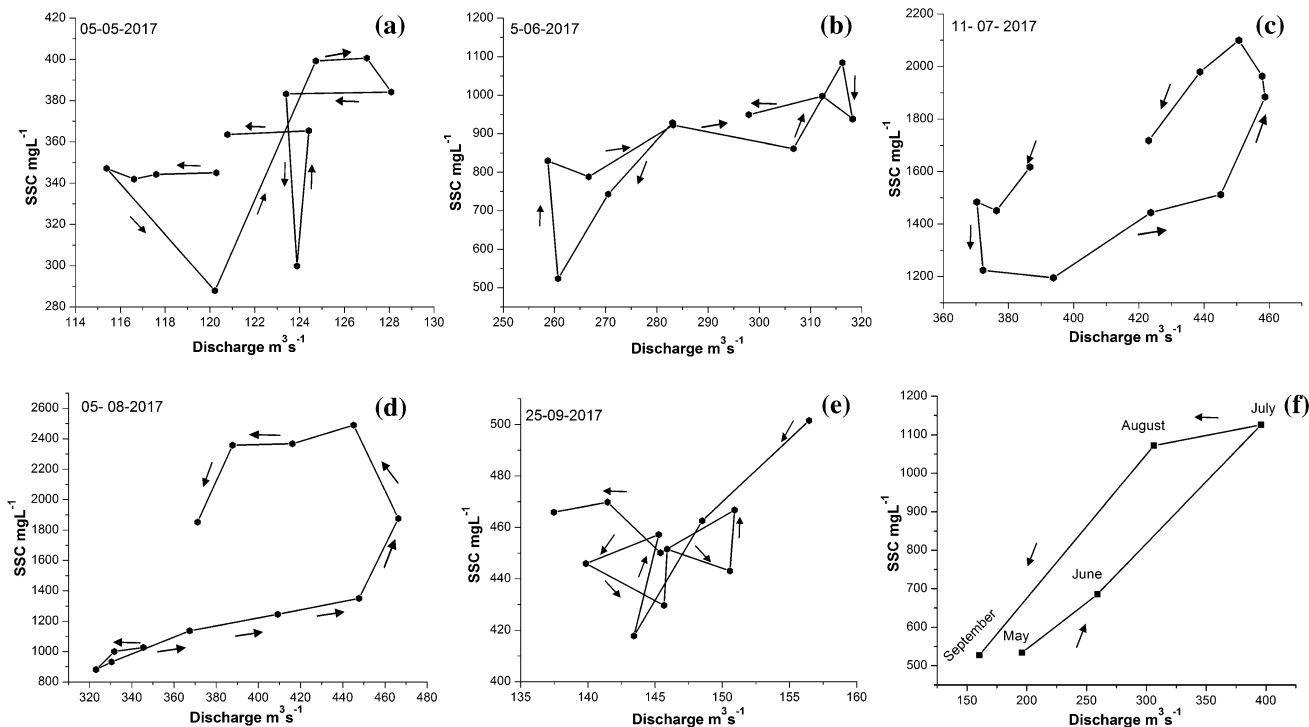
Figure 8. (**a–e**) Diurnal hysteresis for selected days during study period for 2017 ablation period and (**f**) Monthly hysteresis based on monthly mean value for the study period.

Stachnik 2018). Furthermore, dynamic processes like bursting of glacial water pockets, rainstorms, emptying of ice/moraine dammed lakes and other mass movements which are common in high altitude arid terrain may add complexity to hysteresis of the mountainous stream (Tananaev 2015).

The suspended load comprises of different size fractions. The particle size characteristic of SS is its fundamental property controlling the sediment entrainment, transport and deposition in a river. Therefore, grain size analysis of river sediment is significant in understanding sediment provinces and its transport history (Folk and Ward 1957; Haritashya *et al.* 2010). The monthly grain size distribution of SSs is shown in figure 9. Majority of SSs are of silt size particles (85%) followed by sand (8.5%) and clay size particles (6.5 %). Among silt size particles, medium silt is dominant (23.8 ± 2.1%) followed by coarse silt (21.4% ± 2.8), fine silt (17± 1.6%), very coarse silt (13.6 ± 1.6%) and very fine silt (9.1 ± 1.2%). Sand size particles showed the dominance of very fine sand (7.1 ± 2.3%) followed by fine sand (1.4 ± 2.0‰). Clay comprised of rest of the particle size (6.5% ± 0.9). The abundance of various grain sizes follows similar pattern for all months except for fine sand size particles which shows relatively higher concentration in the month of August and completely absent in the
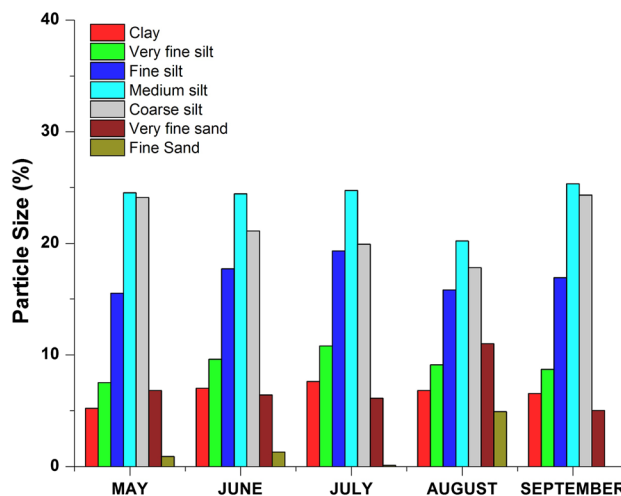

Figure 9. Particle size distribution of the suspended sediment collected from the Chandra River during the 2017 melting season (May–September).

month of September. The total flux of silt, sand, and clay size particles were 2650×10^3, 265×10^3 and 200×10^3 tons yr $^{-1}$, respectively.

The granulometric characteristic of SS of the Chandra River is shown in figure 10. Various SS grain size based statistical parameters such as inclusive graphical median, inclusive graphical mean, inclusive graphic standard deviation,
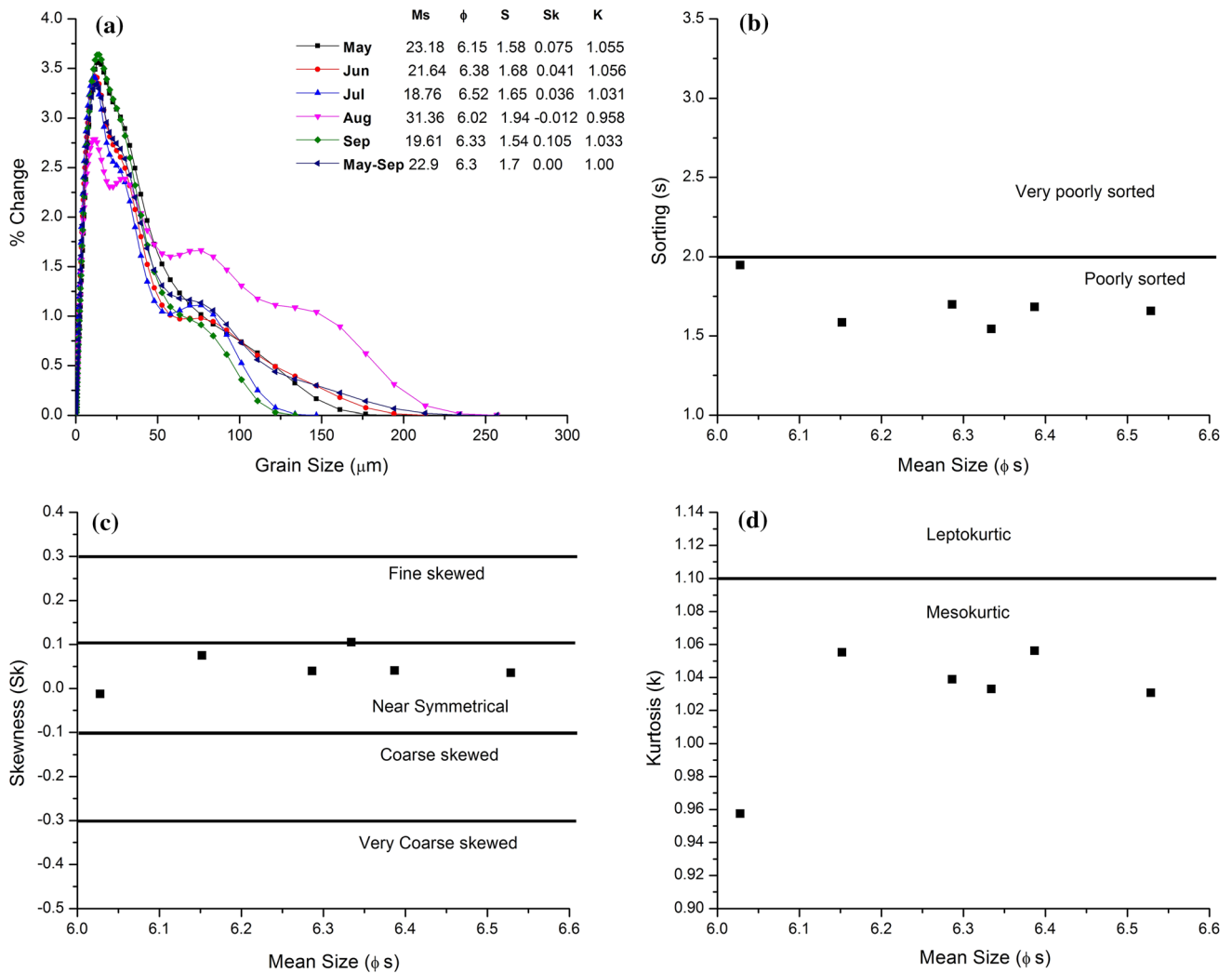
Figure 10. Bivariate plots showing monthly variations in grain size characteristics of Chandra River basin for the 2017 melting season (May–September): (**a**) Grain size distribution for different months, (**b**) Mean size *vs.* sorting, (**c**) Mean size *vs.* skewness, and (**d**) Mean size *vs.* Kurtosis.

inclusive graphic skewness and inclusive graphic kurtosis can be useful to describe sediment characteristics, provenance of the sediments and energy conditions (Folk and Ward 1957). The graphic mean size values for the Chandra River SSs ranged from 6.0 to 6.5ϕ, with a mean value of 6.2ϕ indicating the dominance of medium-grained silt sediments (figure 10a). The graphic mean values are similar to the graphic median value. The medium silt-sized particles could be sourced from the subglacial environment as observed in Chorabari Glacier (Kumar *et al.* 2016) and Gangotri Glacier (Haritashya *et al.* 2010). Inclusive graphic standard deviation (sorting) values varied from 1.5 to 1.9ϕ with an average graphic standard deviation value of 1.68ϕ, reflecting poor sorting of sediments (figure 10b). Such poor sorting values indicate that the sediments were evacuated because of variable

energy conditions during the ablation season in the Chandra Basin. Inclusive graphic skewness varied from –0.01 to 0.10ϕ with an average value of 0.04ϕ (figure 10c). A positive skewness value shows a dominance of fine-sized sediments. Previous studies have shown that if the sediments are of supraglacial origin, they show a coarsely skewed pattern, while finely skewed sediment suggests a subglacial origin of sediments (Kumar *et al.* 2016). Inclusive graphic kurtosis ranged from 0.96 to 1.06 with an average value of 1.02ϕ (figure 10d). These values show equal sorting of tails, and the central part reflects the mesokurtic distribution of sediments. The monthly value remains almost similar throughout the study period. Overall grain size statistics suggest that the SS grains of the Chandra River are poorly sorted medium silt grain size with symmetrical skewness and mesokurtic distribution.

Present study showed a variable pattern of sediment grain size and percentage change along with discharge (table 3). The coarse grain size may increase with discharge in some rivers, while in others fine grain size showed positive relationship with discharge (Walling and Moorehead 1989). However, the grain size in some rivers remain consistent with variable discharge (Walling and Moorehead 1989). In the present study, Principle Component Analysis (PCA) was performed on the monthly dataset of discharge, air temperature, snow cover area and various grain size classes. PCA analysis shows two major components. In component 1 (D1) the finer particle size such as fine silt, very fine silt and clay sized particles showed a positive affinity with the temperature and discharge while snow cover, very coarse silt, coarse silt showed negative relationship with the discharge explaining altogether 54% variability in the data. A negative relationship of coarse silt size particle with discharge suggests that they are dominant in the low flow conditions possibly when the major contribution to the river is derived from the subglacial drainage (Kumar *et al.* 2016). The component D2, explaining 39% variability, consists of relatively coarser particles like fine sand, very fine sand, coarse silt and medium silt. A poor affinity of second component with discharge, snow cover and temperature suggests that they are not governed by energy or meteorological conditions, but controlled by the availability sediments in the system.

A previous study in Chandra River basin by Rao *et al.* (1997) used a different classification method for grain size analysis. They reported that the majority

Table 3. *Principal Component Analysis of monthly mean discharge, temperature and SS particle sizes for the 2017 melting season (May–September). The factor loading >0.5 (bold) indicates a significant association in two principle components.*

Parameter	D1	D2
Discharge	**0.88**	0.29
Temperature	**0.83**	0.42
Snow cover	**−0.67**	0.37
Fine sand	−0.07	**0.99**
V. fine sand	−0.02	**0.98**
V. coarse silt	**−0.92**	0.30
Coarse silt	**−0.63**	**−0.77**
Medium silt	0.01	**−0.99**
Fine silt	**0.88**	−0.44
V. fine silt	**0.99**	−0.15
Clay	**0.97**	0.19
Variability (%)	54.0	39.0
Cumulative (%)	54.0	93.0

of grain size in the Chandra Basin comprises of fine particle size (< 0.075 mm) followed by medium (0.2–0.075 mm) and coarse grain size (>0.2 mm) with percentage contribution of 58, 23.6 and 18.2%, respectively. In comparison to this classification, contribution of fine, medium and coarse grain SS particles in our study were 94, 4.9 and 0.02%, respectively. A significant increase in fine sized sediment is reported in the present study, which could be linked to a significant rise in glacier-melt and rise in river discharge during the past two decades (Tawde *et al.* 2017). In the present study, absence of coarse size particles could be due to lack of their availability. Additionally, significant increase in fine grain size particle could be implied to the comparatively high energy conditions. Most rivers around the world have shown elevated concentration of fine sediment as a result of anthropogenic activities, deforestation, agriculture, construction and mining activities (Owens *et al.* 2005). In the Chandra Basin, a large project like one of longest road tunnel of India 'Atal Tunnel' is under construction since 2010. Furthermore, significant increase in agricultural activities has also been reported in the Lahaul and Spiti district covering the Chandra-Bhaga Basin (Oinam *et al.* 2005). Thus, the impact of anthropogenic activity in promoting the elevated levels of the fine sediment concentration in the Chandra River runoff seems to be significant.

5. Conclusions

Considering the socio-economic importance of the Himalayan region and future warming scenario, the present study attempts to assess the water and suspended sediment (SS) budget of the Chandra River, Western Himalaya. The mean water discharge and SS concentration during ablation period (May–September 2017) in the Chandra River were 260.7 m^3s^{-1} and 775.5 mgL^{-1} with a total water discharge and SS flux of 3536 MCM and 3 million tons, respectively. In comparison to the previous study conducted from 1978 to 1995, we observed a two-fold increase in the SS flux. Heterogeneous hysteresis between river discharge and SS were more common during lean flow conditions while a clear anticlockwise hysteresis was observed during peak flow period. A heterogeneous hysteresis suggests complex drainage through the basin while clear anticlockwise hysteresis indicates open drainage with exhausted sediments or large distance of sediment transport. Overall, the SS were composed of silt size particles

(85%) followed by sand (8.5%) and clay size (6.5%) particles. The SS estimates revealed a total suspended sediment yield of 1285 tons km^{-2} yr^{-1} and physical erosion rate of 0.47 mm yr^{-1}. A significant relationship between discharge, snow cover area, temperature and SS in the present study suggests that in a future warming scenario, the glacierized Himalayan region may report higher water discharge and SS export.

This study provides a high resolution baseline dataset of water discharge, sediment fluxes and aids to understand their dynamics with respect to meteorological conditions in the Chandra Basin. Therefore, considering the present study as a baseline dataset, in future, field and model-based approach can be utilized for long-term assessment of the water resources in the Chandra Basin. The hydro-climatic conditions in the Himalayas region show variable changes, and therefore more studies are required to estimate the discharge, erosion rate and sediment characteristics which will be useful in understanding the SS cycling from the Himalayan region and to build robust models for future projections.

Author statement

ATS, PS, CS, CML, and MT defined the objectives of the study and the writing of the manuscript. ATS and CS have analysed samples for the SSC and grain size at the NCPOR, Goa. LP contributed with plotting the study area map using satellite ArcGIS version 10.4. ATS, LP, SO, and BP supported collecting discharge and meteorological data from the Chandra Basin. All authors contributed to the data interpretation and discussion of the manuscript.

References

Andermann C, Crave A, Gloaguen R, Davy P and Bonnet S 2012 Connecting source and transport: Suspended sediments in the Nepal Himalayas; *Earth Planet. Sci. Lett.* **351** 158–170, https://doi.org/10.1016/j.epsl.2012.06.059.

Arora M, Kumar R, Kumar N and Malhotra J 2014 Assessment of suspended sediment concentration and load from a large Himalayan glacier; *Hydrol. Res.* **45(2)** 292–306, https://doi.org/10.2166/nh.2013.129.

Azam M F, Wagnon P, Vincent C, Ramanathan A L, Favier V, Mandal A and Pottakkal J G 2014 Processes governing the mass balance of Chhota Shigri Glacier (Western Himalaya, India) assessed by point-scale surface energy balance measurements; *Cryosphere* **8(6)** 2195–2217, https://doi.org/10.5194/tc-8-2195-2014.

Pratap B, Sharma P, Patel L, Singh A T, Gaddam V K, Oulkar S and Thamban M 2019 Reconciling high glacier surface melting in summer with air temperature in the semi-arid zone of Western Himalaya; *Water* **11(8)** 1561, https://doi.org/10.3390/w11081561.

Bona F, Doretto A, Falasco E, La Morgia V, Piano E, Ajassa R and Fenoglio S 2016 Increased sediment loads in alpine streams: An integrated field study; *River Res. Appl.* **32(6)** 1316–1326, https://doi.org/10.1002/rra.2941.

Bookhagen B, Thiede R C and Strecker M R 2005 Abnormal monsoon years and their control on erosion and sediment flux in the high, arid northwest Himalaya; *Earth Planet. Sci. Lett.* **231(1–2)** 131–146, https://doi.org/10.1016/j.epsl.2004.11.014.

Chakrapani G J and Saini R K 2009 Temporal and spatial variations in water discharge and sediment load in the Alaknanda and Bhagirathi Rivers in Himalaya, India; *Asian Earth Sci.* **35(6)** 545–553, https://doi.org/10.1016/j.jseaes.2009.04.002.

Davies Colley R J and Smith D G 2001 Turbidity suspended sediment, and water clarity: A review; *J. Am. Water Resour. Assoc.* **37(5)** 1085–1101, https://doi.org/10.1111/j.1752-1688.2001.tb03624.x.

Descloux S, Datry T and Marmonier P 2013 Benthic and hyporheic invertebrate assemblages along a gradient of increasing streambed colmation by fine sediment; *Aquat. Sci.* **75(4)** 493–507, https:// doi.org/https://doi.org/10.1007/s00027-013-0295-6.

Dharmadhikary S 2008 *Mountains of Concrete: Dam Building in the Himalayas*; International Rivers, Berkeley.

Dimri A P, Niyogi D, Barros A P, Ridley J, Mohanty U C, Yasunari T and Sikka D R 2015 Western disturbances: A review; *Rev. Geophys.* **53(2)** 225–246, https://doi.org/10.1002/2014RG000460.

Folk R L and Ward W C 1957 Brazos River bar: A study in the significance of grain size parameters; *J. Sedim. Res.* **27(1)** 3–26, https://doi.org/10.1306/74D70646-2B21-11D7-8648000102C1865D.

Fort M 2000 Glaciers and mass wasting processes: Their influence on the shaping of the Kali Gandaki valley (higher Himalaya of Nepal); *Quat. Int.* **65** 101–119, https://doi.org/10.1016/S1040-6182(99)00039-7.

Geological Survey of India (GSI) 2011 Geological and Mineral Map of Himachal Pradesh; Source: www.gsi.gov.in.

Hall D K and Riggs G A 2016 MODIS/Terra Snow Cover 8-Day L3 Global 500 m SIN Grid, Version 6. Boulder, Colorado USA, NASA National Snow and Ice Data Center, Distributed Active Archive Center.

Haritashya U K, Kumar A and Singh P 2010 Particle size characteristics of suspended sediment transported in meltwater from the Gangotri Glacier, central Himalaya – An indicator of subglacial sediment evacuation; *Geomorphology* **122(1–2)** 140–152, https://doi.org/10.1016/j.geomorph.2010.06.006.

Haritashya U K, Singh P, Kumar N and Gupta R P 2006 Suspended sediment from the Gangotri Glacier: Quantification, variability and associations with discharge and air temperature; *J. Hydrol.* **321 (1)** 116–130, https://doi.org/10.1016/j.jhydrol.2005.07.037.

Iida T, Kajihara A, Okubo H and Okajima K 2012 Effect of seasonal snow cover on suspended sediment runoff in a mountainous catchment; *J. Hydrol.* **428** 116–128, https://doi.org/10.1016/j.jhydrol.2012.01.029.

Immerzeel W W, Van Beek L P H, Konz M, Shrestha A B and Bierkens M F P 2012 Hydrological response to climate change in a glacierized catchment in the Himalayas; *Clim. Change* **110(3–4)** 721–736, https://doi.org/10.1007/s10584-011-0143-4.

Jha P K, Subramanian V and Sitasawad R 1988 Chemical and sediment mass transfer in the Yamuna River – a tributary of the Ganges system; *J. Hydrol.* **104(1–4)** 237–246, https://doi.org/10.1016/0022-1694(88)90167-9.

Kumar A, Gokhale A A, Shukla T and Dobhal D P 2016 Hydroclimatic influence on particle size distribution of suspended sediments evacuated from debris-covered Chorabari Glacier, upper Mandakini catchment, central Himalaya; *Geomorphology* **265** 45–67, https://doi.org/10.1016/j.geomorph.2016.04.019.

Kumar A, Verma A, Gokhale A A, Bhambri R, Misra A, Sundriyal S, Dobhal D P and Kishore N 2018 Hydrometeorological assessments and suspended sediment delivery from a central Himalayan glacier in the upper Ganga basin; *Int. J. Sedim. Res.* **33(4)** 493–509, https://doi.org/10.1016/j.ijsrc.2018.03.004.

Kumar S, Rai H, Purohit K K, Rawat B R S and Mundepi A K 1987 Multi-disciplinary glacier expedition to Chhota Shigri glacier; Department of Science and Technology, Government of India (No. 1, pp. 1–29). New Delhi, Technical Report.

Łepkowska E and Stachnik Ł 2018 Which drivers control the suspended sediment flux in a high arctic glacierized basin (Werenskioldbreen, Spitsbergen); *Water* **10(10)** 1408, https://doi.org/10.3390/w10101408.

Mao L, Comiti F, Carrillo R and Penna D 2019 *Geomorphology of proglacial systems* (eds) Tobias H and David M, Springer International Publishing, pp. 199–217.

Milner A M, Khamis K, Battin T J, Brittain J E, Barrand N E, Fürede L and Hodson A J 2017 Glacier shrinkage driving global changes in downstream systems; *Proc. Natl. Acad. Sci.* **114(37)** 9770–9778, https://doi.org/10.1073/pnas.1619807114.

Oinam S S, Rawat Y S, Khoiyangbam R S, Gajananda K, Kuniyal J C and Vishvakarma S C R 2005 Land use and land cover changes in Jahlma watershed of the Lahaul valley, cold desert region of the northWestern Himalaya, India; *J. Mount. Sci.* **2(2)** 129–136, https://doi.org/10.1007/BF02918328.

Owens P N, Batalla R J, Collins A J, Gomez B, Hicks D M, Horowitz A J and Petticrew E L *et al.* 2005 Fine-grained sediment in river systems: Environmental significance and management issues; *River Res. Appl.* **21(7)** 693–717, https://doi.org/10.1002/rra.878.

Patel L K, Sharma P, Thamban M, Singh A and Ravindra R 2016 Debris control on glacier thinning – a case study of the Batal glacier, Chandra Basin, Western Himalaya; *Arab. J. Geosci.* **9(4)** 309, https://doi.org/10.1007/s12517-016-2362-5.

Rao S V N, Rao M V, Ramasastri K S and Singh R N P 1997 A study of sedimentation in Chenab basin in Western Himalayas; *Hydrol. Res.* **28(3)** 201–216, https://doi.org/10.2166/nh.1997.0012.

Sharma P, Patel L K, Ravindra R, Singh A, Mahalinganathan K and Thamban M 2016 Role of debris cover to control specific ablation of adjoining Batal and Sutri Dhaka glaciers in Chandra Basin (Himachal Pradesh) during peak ablation season; *J. Earth Syst. Sci.* **125(3)** 459–473, https://doi.org/10.1007/s12040-016-0681-2.

Singh A T, Laluraj C M, Sharma P, Patel L K and Thamban M 2017 Export fluxes of geochemical solutes in the meltwater stream of Sutri Dhaka Glacier, Chandra Basin, Western Himalaya; *Environ. Monit. Assess.* **189(11)** 555, https://doi.org/10.1007/s10661-017-6268-9.

Singh A T, Rahaman W, Sharma P, Laluraj C M, Patel L K, Pratap B and Thamban M 2019 Moisture sources for precipitation and hydrograph components of the Sutri Dhaka Glacier Basin, Western Himalayas; *Water* **11(11)** 2242, https://doi.org/10.3390/w11112242.

Singh V B and Ramanathan A L 2018 Suspended sediment dynamics in the meltwater of Chhota Shigri glacier, Chandra basin, Lahaul-Spiti valley, India; *J. Mt. Sci.* **15(1)** 68–81, https://doi.org/10.1007/s11629-017-4554-1.

Singh V B, Ramanathan A L, Pottakkal J G and Kumar M 2014 Seasonal variation of the solute and suspended sediment load in Gangotri glacier meltwater, central Himalaya, India; *J Asian Earth Sci.* **79** 224–234, https://doi.org/10.1016/j.jseaes.2013.09.010.

Srivastava D, Kumar A, Verma A and Swaroop S 2014 Characterization of suspended sediment in meltwater from glaciers of Garhwal Himalaya; *Hydrol. Process.* **28(3)** 969–979, https://doi.org/10.1002/hyp.9631.

Subramanian V 1993 Sediment load of Indian rivers; *Curr. Sci.* 928–930.

Subramanian V 1996 The sediment load of Indian rivers – an update; IAHS Publications-Series of Proceedings and Reports; *Int. Assoc. Hydrol. Sci.* **236** 183–190.

Tananaev N I 2015 Hysteresis effects of suspended sediment transport in relation to geomorphic conditions and dominant sediment sources in medium and large rivers of the Russian Arctic; *Hydrol. Res.* **46(2)** 232–243, https://doi.org/10.2166/nh.2013.199.

Tawde S A, Kulkarni A V and Bala G 2017 An estimate of glacier mass balance for the Chandra Basin, Western Himalaya, for the period 1984–2012; *Ann. Glaciol.* **58** 99–109, https://doi.org/10.1017/aog.2017.18.

Udden J A 1914 Mechanical composition of clastic sediments; *Bull. Geol. Soc. Am.* **25(1)** 655–744, https://doi.org/10.1130/GSAB-25-655.

Walling D E and Moorehead P W 1989 The particle size characteristics of fluvial suspended sediment: An overview; In: *Sediment/Water Interactions. Developments in Hydrobiology* (eds) Sly P G and Hart B T, vol 50, Springer, Dordrecht, https://doi.org/10.1007/978-94-009-2376-8_12.

Wulf H, Bookhagen B and Scherler D 2012 Climatic and geologic controls on suspended sediment flux in the Sutlej River Valley, western Himalaya; *Hydrol. Earth Syst. Sci.* **16(7)** 2193–2217, https://doi.org/10.5194/hess-16-2193-2012.

Corresponding editor: C GNANASEELAN